Japan Architectural Review
Open Access
Architectural Institute of Japan

Translated Paper

Critical earthquake response of a SDOF elastic-perfectly plastic model with viscous damping under double impulse as a substitute for near-fault ground motion

Kotaro Kojima,[1] Yoshito Saotome[2] and Izuru Takewaki[1]

[1]Department of Architecture and Architectural Engineering, Kyoto University, Kyoto, Japan; [2]School of Architecture, Kyoto University, Kyoto, Japan

Correspondence
Izuru Takewaki, Department of Architecture and Architectural Engineering, Kyoto University, Kyoto, Japan.
Email: takewaki@archi.kyoto-u.ac.jp

Funding information
Japan Society for the Promotion of Science (Grant Number: KAKENHI/No. 15H04079, 15J00960).

The Japanese version of this paper was published in Volume 82, Number 735, pages 643-652, https://doi.org/10.3130/aijs.82.643 of *Journal of Structural and Construction Engineering (Transactions of AIJ)*. The authors have obtained permission for secondary publication of the English version in another journal from the Editor of *Journal of Structural and Construction Engineering (Transactions of AIJ)*. This paper is based on the translation of the Japanese version with some slight modifications.

Received August 30, 2017; Accepted November 7, 2017

doi: 10.1002/2475-8876.10019

Abstract

The double-impulse input is introduced as a substitute for the fling-step near-fault ground motion, and a closed-form solution for the approximate elastic-plastic response of a structure with viscous damping under the "critical double impulse" is derived. Since only the free vibration appears under such a double impulse, the energy approach plays an important role in the derivation of the closed-form solution for a complicated elastic-plastic response with viscous damping. The quadratic function approximation for the damping force-deformation relationship is introduced. The validity and accuracy of the proposed theory are investigated through comparison of the results of the response analysis to the corresponding one-cycle sinusoidal input and actual recorded ground motions.

Keywords
critical earthquake response, double impulse, elastic-plastic response, near-fault ground motion, quadratic function approximation, viscous damping

1. Introduction

After large earthquake events, such as the Parkfield earthquake in 1966, the San Fernando earthquake in 1971, the Northridge earthquake in 1994, the Hyogoken-Nanbu (Kobe) earthquake in 1995 and the Chi-Chi (Taiwan) earthquake in 1999, various aspects of near-fault ground motions have been clarified. A near-fault ground motion is characterized by a few series of pulse-like wavelets, and the effects of near-fault ground motions on structural response have been investigated extensively.[1-5] In recent papers, fling-step and forward-directivity inputs have been characterized by two or three sinusoidal wavelets.[1,4,6,7]

In the previous studies, it was noted that such pulse-like ground motions cause large deformations in elastic-plastic structures, and it was made clear that the maximum response under a pulse-like ground motion is related to the ratio of the period of the pulse-like ground motion to the fundamental natural period of the structure. Minami and Hayashi reduced a multi-story building structure to a shear beam model and showed that the number of modes to be included for representing the deformation concentration differs depending on the ratio of the period of the pulse-like ground motion to the fundamental natural period of the structure.[8]

Although not limited to near-fault ground motions, some effective methods that represent the ground motion as a one-cycle sinusoidal wave have been proposed.[9,10] Sakai et al. showed that the elastic-plastic response under such ground motion can be expressed by using the maximum ground acceleration and the effective period.[9] In other studies, the response characteristics under impulsive ground motions were clarified from the viewpoint of energy input per half-cycle.[11,12]

Most of the previous works on near-fault ground motions using the half-cycle sinusoidal wave or wavelets address the elastic response because the number of parameters (e.g., duration and

amplitude of pulse, ratio of pulse frequency to structure natural frequency) to be considered on this topic is large. In the previous studies on treating the elastic-plastic response, the responses were calculated numerically by using time-history response analysis.

Kojima and Takewaki introduced a double impulse or a triple impulse as a substitute for the one-cycle sinusoidal wave or 1.5-cycle sinusoidal wave for representing the main part of the near-fault ground motion and derived the closed-form expression of the elastic-plastic response of the undamped single-degree-of-freedom (SDOF) elastic-perfectly plastic system and the undamped SDOF bilinear hysteretic system under the critical double impulse (or the critical triple impulse).[13-16] The Fourier amplitude of the double impulse and the triple impulse is similar to that of the one-cycle sinusoidal wave and the 1.5-cycle sinusoidal wave in a certain frequency range, and the maximum Fourier amplitude of the double impulse and the triple impulse was adjusted to that of the one-cycle sinusoidal wave and the 1.5-cycle sinusoidal wave. Since the response under the impulse can be expressed by the instantaneous change in the velocity of the structural mass and only the free vibration appears after the impulse input, the closed-form expression of a complicated elastic-plastic response can be derived in a simple manner by using the energy balance law. In particular, this approach focuses on finding the critical timing that maximizes the peak deformation and this theory is based on the concept of "critical excitation."[17,18] The second impulse of the critical double impulse acts at the zero restoring force timing after the first impulse (at this timing the velocity of the undamped system attains its maximum). Therefore, the closed-form expression of the resonant input period (the critical time interval of the double impulse) can also be derived by using the double impulse. Although the resonant response and the resonant equivalent frequency of the elastic-plastic system under the sinusoidal input must be computed for a specified input level by changing the excitation frequency in a parametric manner when using the equivalent linearization method[19,20] or time-history response analysis, the critical response and the critical time interval of the elastic-plastic system can be obtained directly without the repetitive procedure when using the proposed method. The closed-form expression of the uncritical response can also be obtained by using the analytical solution of free vibration that corresponds to the initial condition.

In this study, the closed-form expression of the maximum deformation of the undamped SDOF elastic-perfectly plastic system under the critical double impulse is extended to a SDOF system with both viscous damping and the elastic-perfectly plastic restoring force characteristic. Once the present study has been completed, the critical excitation theory for the elastic-plastic system can be used for vibration control and base-isolation structures including additional damping. However, it may be difficult to obtain the analytical solution for the response of a system with both viscous damping and elastic-plastic hysteretic damping when solving the differential equation, even by using the double impulse. Therefore, quadratic function approximation of the damping force-deformation relation is introduced here. The work done by the damping force can be evaluated simply by using the quadratic function approximation, and the closed-form maximum elastic-plastic response can be derived approximately by using the energy balance law and the assumption of the critical timing. The accuracy of the quadratic function approximation of the damping force-deformation relation and the validity of the assumption of the critical timing are investigated by using time-history response analysis.

It may be possible to design a building with high robustness and redundancy by evaluating the worst-case response (critical response) to near-fault ground motion. Although the maximum ground velocity is given as a specified index of ground motions in the current structural design procedure of high-rise buildings and base-isolated buildings, the characteristic period of ground motions is extremely uncertain. Therefore, it may be possible to design a building with higher safety by evaluating the critical elastic-plastic response with variable ground motion period for the specific input level.

2. Modeling of near-fault ground motion with a double impulse

The fling-step input (fault-parallel) of a near-fault ground motion can be characterized by a one-cycle sinusoidal wave, and the forward-directivity input (fault-normal) can be characterized by a series of three sinusoidal wavelets as shown in Figure 1.[6,7] The double impulse and the triple impulse were introduced as substitutes for the fling-step input and the forward-directivity input in the previous papers.[13-16] In this paper, the double impulse is used. The critical time interval in the double impulse for the undamped system (with corresponds to the resonant frequency in the one-cycle sinusoidal wave) can be obtained directly. In contrast, the resonant frequency of the one-cycle sinusoidal wave has to be computed for a specified input level by changing the input frequency in a parametric manner and transforming the structural model in the conventional approach.[19,20]

A ground acceleration $\ddot{u}_g(t)$ in terms of the double impulse is expressed by

$$\ddot{u}_g(t) = V\delta(t) - V\delta(t - t_0), \tag{1}$$

where V is the given initial velocity (the input velocity of each impulse), t_0 is the time interval between two impulses and $\delta(t)$ is the Dirac delta function. The comparison of the double impulse with the corresponding one-cycle sinusoidal wave is shown in Figure 1A. The Fourier transform of $\ddot{u}_g(t)$ of the double impulse can be derived as

$$\ddot{U}_g(t) = \int_{-\infty}^{\infty} \{V\delta(t) - V\delta(t - t_0)\} e^{-i\omega t} dt = V(1 - e^{-i\omega t}), \tag{2}$$

where i denotes the imaginary unit.

It is necessary to adjust the input level of the double impulse to that of the one-cycle sinusoidal wave for the comparison of the elastic-plastic responses. In this paper, the input level of the double impulse and the one-cycle sinusoidal wave is adjusted based on the equivalence of the maximum Fourier amplitude.[13,15,16] The validity of this adjustment method has been shown for undamped bilinear hysteretic and elastic-perfectly plastic systems.[13,15,16] The ratio of the maximum ground velocity V_p of the one-cycle sinusoidal wave to the input velocity level of the double impulse can be shown to be constant by using the adjustment method based on the equivalence of the Fourier amplitude.[16] Therefore, the one-cycle sinusoidal wave that corresponds to the double impulse based on the equivalence of the Fourier amplitude can be obtained as follows.

$$\ddot{u}_g^{SW}(t) = 0.5\omega_p V_p \sin(\omega_p t) \quad (0 \le t \le T_p = 2t_0), \tag{3}$$

where $V_p/V = 1.2222$,[16] and T_p and $\omega_p = 2\pi/T_p$ denote the period and the circular frequency, respectively, of the corresponding one-cycle sinusoidal wave. The relation between the time

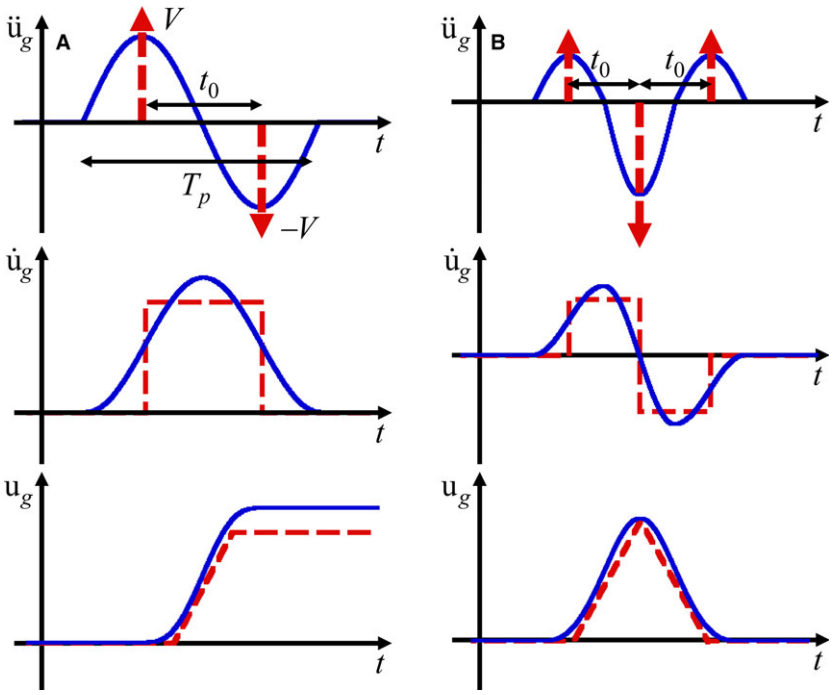

Figure 1. Modeling of near-fault ground motion: (A) Fling-step input and double impulse, (B) Forward-directivity input and triple impulse

interval t_0 and the period T_p is $T_p = 2t_0$. The starting times of the double impulse and the corresponding one-cycle sinusoidal wave differ by $t_0/2$, as shown in Figure 1A. This difference does not affect the Fourier amplitude of the one-cycle sinusoidal wave. The one-cycle sinusoidal wave that is defined in Equation (3) is used for verification of the closed-form expression of the elastic-plastic response under the critical double impulse.

3. SDOF elastic-perfectly plastic system with viscous damping

Consider an SDOF elastic-perfectly plastic system of mass m, stiffness k, and damping coefficient c. The damping coefficient is constant, regardless of yielding. $\omega_1 = \sqrt{k/m}$, $T_1 = 2\pi/\omega_1$ and $h = c/(2\sqrt{km})$ denote the undamped natural circular frequency, the undamped natural period, and the damping ratio, respectively. $\omega_1' = \sqrt{1-h^2}\omega_1$ and $T_1' = 2\pi/\omega_1'$ denote the damped natural circular frequency and the damped natural period, respectively. u, f_R, and f_D are the displacement of the mass relative to the ground (deformation of the system), the restoring force of the model, and the damping force, respectively. d_y and f_y denote the yield deformation and the yield force. These parameters will be treated as normalized parameters to capture the intrinsic relation between the input parameters and the elastic-plastic response.

4. Elastic-perfectly plastic response of the undamped system under the critical double impulse

Kojima and Takewaki have derived a closed-form expression of the elastic-perfectly plastic response of an undamped SDOF system under the critical double impulse.[13] The maximum elastic-plastic responses of the undamped SDOF system under the critical double impulse can be derived by an energy approach without solving directly the equation of motion. In other words, the maximum deformation can be calculated by using the energy balance law, in which the kinetic energies given at the times of the first impulse and the second impulse are transformed into the sum of the elastic strain energy corresponding to the yield deformation and the energy dissipated during the plastic deformation. The critical elastic-plastic response can be derived in closed form, and the critical time interval (corresponding to a half of the resonant period) can be derived automatically for the increasing input velocity level of the double impulse by using this method. Since a similar theory can be developed for deriving the elastic-plastic response of a damped SDOF system, the closed-form expression of the maximum deformation of the undamped elastic-perfectly plastic system that was derived in the previous paper[13] is explained briefly in this section.

The maximum deformations after the first impulse and the second impulse are denoted by $u_{\max 1}$ and $u_{\max 2}$ ($u_{\max 1}$ and $u_{\max 2}$ are the absolute values), respectively, as shown in Figure 2, and the maximum deformation under the critical double impulse is evaluated by $u_{\max} = \max(u_{\max 1}, u_{\max 2})$. The plastic deformations after the first impulse and the second impulse are denoted by u_{p1} and u_{p2}, respectively. The maximum elastic-perfectly plastic response of the undamped SDOF system under the critical double impulse can be classified into one of three cases, depending on the input velocity level (yielding stage). CASE 1 is the case of elastic response even after the second impulse. CASE 2 is the case of plastic deformation only after the second impulse. CASE 3 is the case of plastic deformation after the first impulse. Figure 2 shows a schematic diagram of CASE 1, CASE 2, and CASE 3. Let $V_y(=\omega_1 d_y)$ denote the input velocity level of the double impulse at which the maximum deformation of the undamped SDOF system just attains the yield deformation after the first impulse: this parameter is a strength parameter of the SDOF system. V_y is used for normalizing the input velocity level, and V/V_y is simply called the input velocity level. $u_{\max 1}$ and $u_{\max 2}$ with respect to V/V_y in CASES 1–3 can be obtained as follows by using the energy balance law.

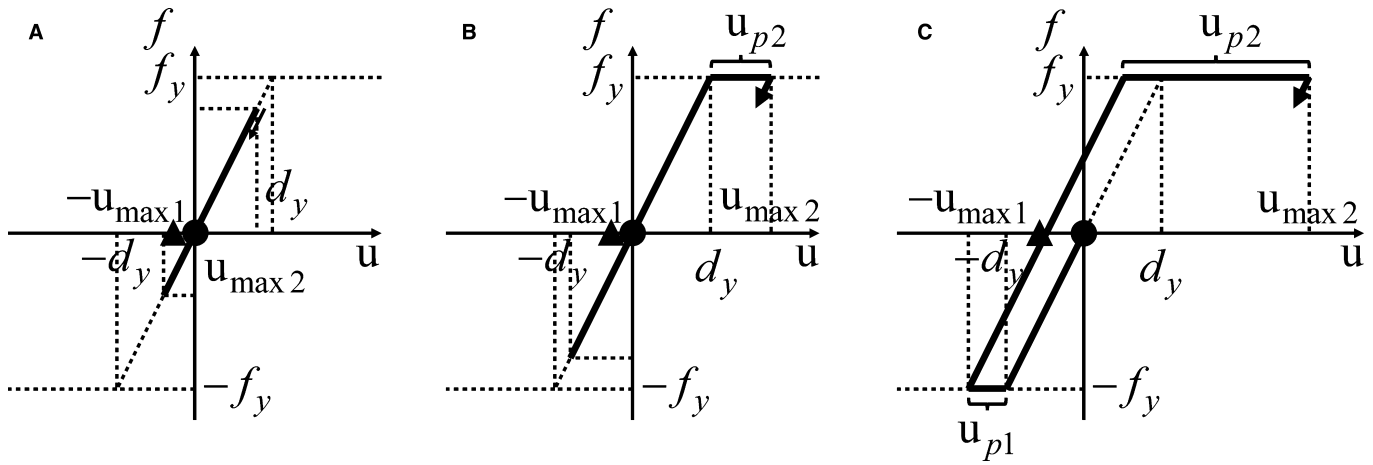

Figure 2. Maximum deformation of the elastic-perfectly plastic model under the critical double impulse: (A) CASE 1: elastic range, (B) CASE 2: yielding after 2nd impulse, (C) CASE 3: yielding after 1st impulse (●: 1st impulse, ▲: 2nd impulse)

$$\frac{u_{\max 1}}{d_y}=\begin{cases} V/V_y & \text{for } 0\le V/V_y<1.0 \quad (\text{CASE}1,2) \\ 0.5\{1+(V/V_y)^2\} & \text{for } 1.0\le V/V_y \quad (\text{CASE}3) \end{cases} \tag{4}$$

$$\frac{u_{\max 2}}{d_y}=\begin{cases} 2V/V_y & \text{for } 0\le V/V_y<0.5 \quad (\text{CASE}1) \\ 0.5\left\{1+(2V/V_y)^2\right\} & \text{for } 0.5\le \frac{V}{V_y}<1.0 \quad (\text{CASE}2) \\ 1.5+(V/V_y) & \text{for } 1.0\le V/V_y \quad (\text{CASE}3) \end{cases} \tag{5}$$

Figure 3 shows the maximum deformation of the undamped SDOF elastic-perfectly plastic system under the critical double impulse normalized by the yield deformation with respect to input velocity level V/V_y. The critical timing of the second impulse (the critical time interval), which maximizes the maximum deformation u_{max2} after the second impulse, is characterized as the time when the restoring force is zero in the unloading process after the first impulse.[13] In CASES 1 and 2, since the response after the first impulse is in an elastic range, the critical time interval t_0^c is half of the initial natural period T_1 of the SDOF system. In CASE 3, since the SDOF system enters the yielding stage after the first impulse, it is necessary to derive the expression by solving the equation of motion. The critical time interval t_0^c can be obtained by solving the equation of motion as follows.

$$\frac{{t_0}^c}{T_1}=\begin{cases} 0.5 & \text{for } 0\le V/V_y<1.0 \quad (\text{CASE}\,1,2) \\ \left\{\arcsin(V_y/V)+\sqrt{(V/V_y)^2-1}\right\}/(2\pi)+1/4 & \\ \text{for } 1.0\le V/V_y \quad (\text{CASE}\,3) & \end{cases} \tag{6}$$

Figure 4 shows the critical time interval t_0^c, normalized by T_1, with respect to input velocity level V/V_y.

5. Linear elastic response of the damped system under the critical double impulse

In this section, a closed-form expression for the maximum deformation of an elastic SDOF system with viscous damping under the critical double impulse is derived to investigate the effect of viscous damping on the response under the double impulse.

Since the response of the linear elastic SDOF system after the second impulse can be obtained by simply superposing the free vibrations after the first impulse and the second impulse, the deformation response and the velocity response after the first impulse and the second impulse can be obtained, respectively, with respect to general time interval t_0 as follows.

$$u(t) = -(V/\omega_1')e^{-h\omega_1 t}\sin(\omega_1' t) \quad (t<t_0), \tag{7a}$$

$$\dot{u}(t)=-(V/\sqrt{1-h^2})e^{-h\omega_1 t}\cos(\omega_1' t+\phi) \quad (t<t_0), \tag{7b}$$

$$\begin{aligned} u(t)&=-\frac{V}{\omega_1'}e^{-h\omega_1 t}\sin(\omega_1' t)+\frac{V}{\omega_1'}e^{-h\omega_1(t-t_0)}\sin\{\omega_1'(t-t_0)\} \\ &=-\frac{V}{\omega_1'}\sqrt{1-2e^{h\omega_1 t_0}\cos(\omega_1' t_0)+e^{2h\omega_1 t_0}}e^{-h\omega_1 t}\sin(\omega_1' t+\theta) \end{aligned} \quad (t\ge t_0), \tag{8a}$$

$$\begin{aligned} \dot{u}(t) = &-V\sqrt{\frac{1-2e^{h\omega_1 t_0}\cos(\omega_1' t_0)+e^{2h\omega_1 t_0}}{1-h^2}}e^{-h\omega_1 t} \\ &\cos(\omega_1' t+\theta+\phi) \quad (t\ge t_0), \end{aligned} \tag{8b}$$

where

$$\phi=\arctan(h/\sqrt{1-h^2}), \tag{9a}$$

$$\theta=\begin{cases} \arctan\frac{e^{h\omega_1 t_0}\sin(\omega_1' t_0)}{1-\exp(h\omega_1 t_0)\cos(\omega_1' t_0)} & \left(1-e^{h\omega_1 t_0}\cos(\omega_1' t_0)\ge 0\right) \\ \arccos\frac{1-e^{h\omega_1 t_0}\cos(\omega_1' t_0)}{\sqrt{1-2e^{h\omega_1 t_0}\cos(\omega_1' t_0)+e^{2h\omega_1 t_0}}} & \begin{pmatrix} 1-e^{h\omega_1 t_0}\cos(\omega_1' t_0)<0 \\ \text{and } e^{h\omega_1 t_0}\sin(\omega_1' t_0)\ge 0 \end{pmatrix} \\ -\arccos\frac{1-e^{h\omega_1 t_0}\cos(\omega_1' t_0)}{\sqrt{1-2e^{h\omega_1 t_0}\cos(\omega_1' t_0)+e^{2h\omega_1 t_0}}} & \begin{pmatrix} 1-e^{h\omega_1 t_0}\cos(\omega_1' t_0)<0 \\ \text{and } e^{h\omega_1 t_0}\sin(\omega_1' t_0)<0 \end{pmatrix} \end{cases}. \tag{9b}$$

The deformation responses after the first impulse and the second impulse are maximized at the time at which $\dot{u}=0$. The

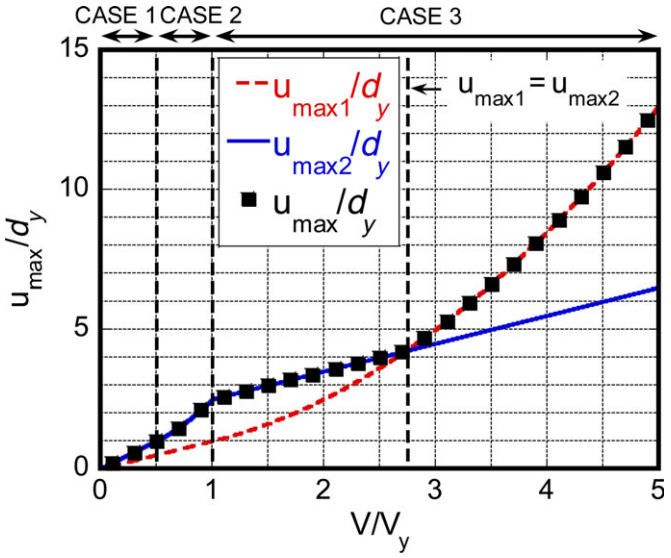

Figure 3. Maximum deformation u_{max}/d_y for input level V/V_y[13]

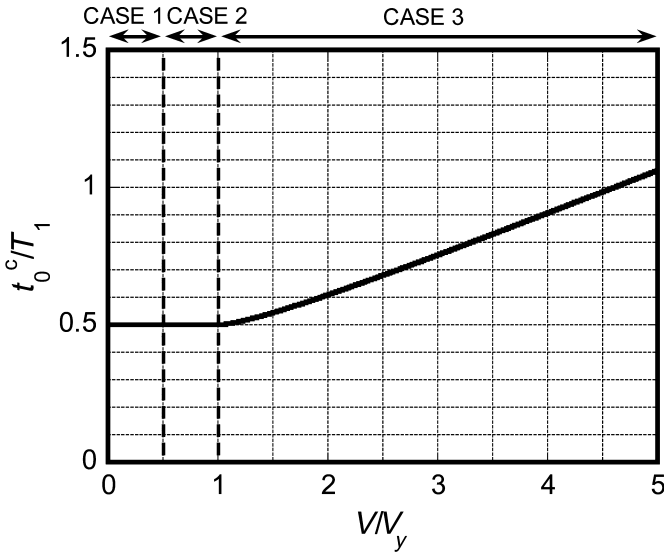

Figure 4. Critical impulse timing t_0^c/T_1 for input level V/V_y[13]

maximum deformations u_{max1} and u_{max2} (absolute values) after the first impulse and the second impulse, respectively, can be obtained as follows.

$$u_{max\,1} = \begin{cases} (V/\omega_1')\exp(-h\omega_1 t_0)\sin(\omega_1' t_0) & (t_0 < t_{max\,1}) \\ (V/\omega_1')\exp(-h\omega_1 t_{max\,1})\sin(\omega_1' t_{max\,1}) & (t_0 \geq t_{max\,1}) \end{cases}, \tag{10a}$$

$$u_{max\,2} = \frac{-V}{\omega_1'} e^{-h\omega_1 t_{max\,2}} \sqrt{1 - 2e^{h\omega_1 t_0}\cos(\omega_1' t_0) + e^{2h\omega_1 t_0}} \sin(\omega_1' t_{max\,2} + \theta), \tag{10b}$$

where

$$t_{max\,1} = \{0.25 - \phi/(2\pi)\}T_1', \tag{11a}$$

$$t_{max\,2} = \{(4N-1)/4 - (\theta+\phi)/(2\pi)\}T_1'. \tag{11b}$$

N is a positive integer satisfying $N - 1 \leq (t_0/T_1') < N$.

From Equations (10a), (10b), (11a), and (11b), the relation between the time interval t_0 and the maximum deformation $u_{max} = \max(u_{max1}, u_{max2})$ can be obtained explicitly. Figure 5 shows the maximum deformation $u_{max} = \max(u_{max1}, u_{max2})$ with respect to the time interval t_0 for various damping ratios h = 0.01,0.02,0.05,0.1,0.2,0.5. The abscissa is the time interval t_0, normalized by the critical time interval t_0^c, and the ordinate is the maximum deformation u_{max}, normalized by $2V/\omega_1$, which is the maximum deformation of the undamped SDOF system under the critical double impulse. The critical time interval of the elastic SDOF system is $t_0^c = T_1'/2$. This can be proved by setting $du_{max\,2}/dt_0|_{t_0 = t_0^c} = 0$ (see Appendix 1), and the restoring force is zero at the time $t = T_1'/2$ after the first impulse (the first impulse acts at the time t = 0). One should ensure that the velocity response of the damped SDOF system does not attain the maximum at the critical timing (the zero restoring force timing) after the first impulse. The maximum deformation u_{max1}, u_{max2} of the elastic SDOF system with viscous damping under the critical double impulse can be obtained as follows by substituting $t_0 = T_1'/2$ into Equations (10a), (10b), (11a) and (11b).

$$u_{max\,1} = \frac{V}{\omega_1}\exp\left\{-\frac{h}{\sqrt{1-h^2}}\left(\frac{\pi}{2} - \arctan\frac{h}{\sqrt{1-h^2}}\right)\right\} \tag{12a}$$

$$u_{max\,2} = \frac{V}{\omega_1}\exp\left\{-\frac{h}{\sqrt{1-h^2}}\left(\frac{3}{2}\pi - \arctan\frac{h}{\sqrt{1-h^2}}\right)\right\}\left\{1 + \exp\left(\frac{\pi h}{\sqrt{1-h^2}}\right)\right\} \tag{12b}$$

Figure 6 presents a comparison of the maximum deformation under the double impulse with respect to the time interval t_0 and the maximum deformation under the corresponding one-cycle sinusoidal wave with respect to the input period T_p. The damping ratios are taken as h = 0.05,0.2 in Figure 6. The input period T_p is changed for the specific maximum velocity calculated by $V_p = 1.2222V$ with the input velocity level V. The critical input period T_p^c is double the critical time interval t_0^c because of the correspondence between the double impulse and the one-cycle sinusoidal wave. The abscissa $t_0/t_0^c (= T_p/T_p^c)$ for the corresponding sinusoidal wave denotes the input period T_p, normalized by the approximate critical period $T_p^c (= 2t_0^c)$. Although the maximum deformation under the corresponding one-cycle sinusoidal wave is maximized at a period that is slightly shorter than the critical input period T_p^c that is calculated by using the critical double impulse, the maximum deformation under the critical double impulse is in good correspondence with the upper bound of the maximum deformation under the corresponding one-cycle sinusoidal wave.

6. Elastic-plastic response of the damped system under the critical double impulse

6.1 Approximate critical response of the elastic-plastic system with viscous damping based on the energy balance law

In this section, a closed-form expression is derived for the maximum deformation of the elastic-perfectly plastic system with viscous damping under the critical double impulse. The

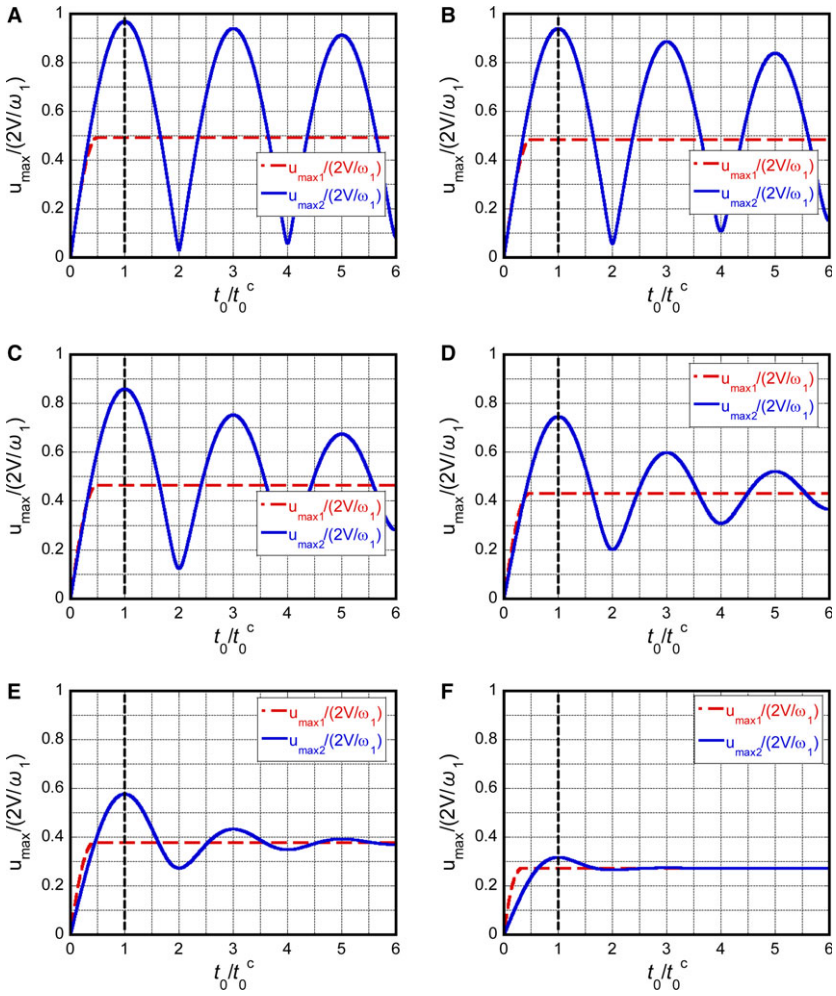

Figure 5. Maximum elastic deformation u_{max}/d_y with viscous damping under the double impulse for varied impulse timing: (A) $h = 0.01$, (B) $h = 0.02$, (C) $h = 0.05$, (D) $h = 0.1$, (E) $h = 0.2$, (F) $h = 0.5$

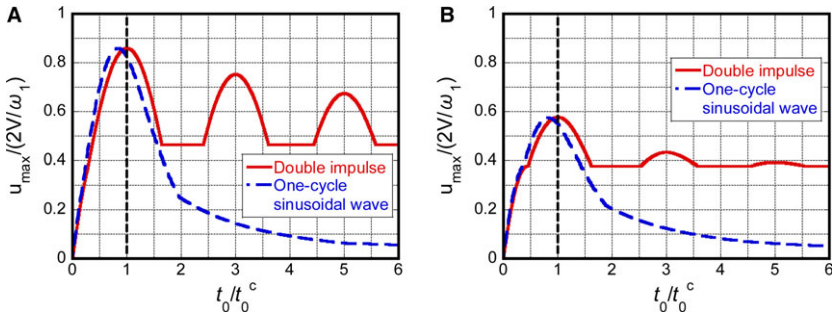

Figure 6. Comparison of maximum elastic deformation u_{max}/d_y with viscous damping under the double impulse and the equivalent one-cycle sine wave for varied impulse timing: (A) $h = 0.05$, (B) $h = 0.2$

maximum deformation of the undamped elastic-perfectly plastic system under the critical double impulse can be evaluated by using the energy balance law, in which the kinetic energies given at the time of the first impulse and the second impulse are transformed into the sum of the hysteretic energy and the maximum elastic strain energy corresponding to the yield deformation. In the elastic-plastic system with viscous damping, the kinetic energies given at the first impulse and the second impulse are equal to the sum of the elastic strain energy corresponding to the yield deformation, the energy dissipated during the plastic deformation and the work done by the damping force (the energy consumed by viscous damping). This corresponds to the energy balance law for the elastic-plastic system with viscous damping (Figure 7). However, it is difficult to obtain the exact analytical solution for the response of the system with both hysteretic damping and viscous damping by solving the differential equation, even by using a simple input such as a double impulse. In this study, a method is

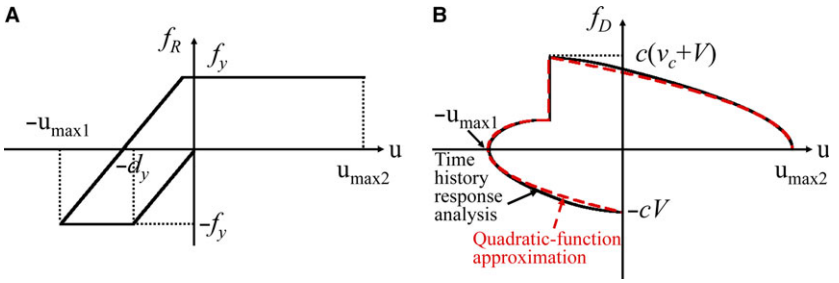

Figure 7. Quadratic approximation of damping force-deformation relation and its application to evaluation of maximum deformation of the elastic-perfectly plastic model with viscous damping: (A) Restoring force-deformation relation, (B) Damping force-deformation relation

developed for approximating the damping force-deformation relation by using a quadratic function whose vertex is at the zero-velocity point (the point of maximum displacement). A quadratic function that passes through both the acting point of the first or second impulse, and the zero-velocity point may be the simplest function that can represent the behavior of the damping force-deformation relation near the zero-velocity point. Using this approximation, the work done by the damping force can be represented by using the damping force that is calculated based on the initial velocity (the velocity just after the first or second impulse) and the maximum deformation.

According to Sections 4 and 5, the critical timing of the second impulse of both the linear elastic system with viscous damping and the undamped elastic-plastic system is the zero restoring force timing in the unloading process after the first impulse. Therefore, it can be assumed that the critical timing of the second impulse of the elastic-plastic system with viscous damping is also the zero restoring force timing in the unloading process after the first impulse. The validity of this assumption will be investigated numerically in Section 6.5. In this section, the closed-form expression is derived approximately for the maximum deformation of the SDOF elastic-perfectly plastic system with viscous damping under the critical double impulse by using (i) the quadratic function that approximates the damping force-deformation relation, (ii) the assumption that the zero restoring force timing is the critical timing of the second impulse and (iii) the energy balance law for the elastic-plastic system with viscous damping. Furthermore, the accuracy of the quadratic function approximation for the damping force-deformation relation and the validity of the assumption that the zero restoring force timing is the critical timing of the second impulse are investigated by using time-history response analysis.

The maximum deformations after the first impulse and the second impulse are denoted by u_{max1} and u_{max2} (u_{max1} and u_{max2} are the absolute values), respectively, as shown in Figure 7, and the maximum deformation under the critical double impulse is evaluated by $u_{max} = \max(u_{max1}, u_{max2})$. The elastic-plastic response of the SDOF elastic-perfectly plastic system with viscous damping under the critical double impulse can be classified into one of three cases, depending on the input velocity level. CASE 1 is the case of elastic response, even after the second impulse. CASE 2 is the case of plastic deformation only after the second impulse. CASE 3 is the case of plastic deformation after the first impulse. Figure 8 shows a schematic diagram of CASE 1, CASE 2, and CASE 3. In this section, V_y is equal to $V_y(=\omega_1 d_y)$, as defined in Section 4.

6.2 CASE 1: Elastic response even after second impulse

First, consider CASE 1, which is the case of the elastic response, even after the second impulse. Figure 8A shows the evaluation process of the maximum deformations u_{max1}, u_{max2} after the first impulse and the second impulse, respectively, for the elastic case (CASE 1). Although the exact solution for the elastic response of the system with viscous damping was derived in Section 5, an approximate closed-form solution of the maximum deformation is derived here by using the quadratic function approximation for the damping force-deformation relation. The approximate solution that is derived in this section is a good approximation of the exact solution that was obtained in Section 5.

The work done by the damping force after the first impulse is derived by using the quadratic function approximation for the damping force-deformation relation. The damping force-deformation relation after the first impulse is approximated by a quadratic function with vertex $(u, f_D) = (-u_{max1}, 0)$ and passing through the point $(u, f_D) = (0, -cV)$. f_D can be obtained as follows.

$$f_D = -cV\sqrt{1+(u/u_{max\,1})} \tag{13}$$

The work done by the damping force can be obtained by integrating Equation (13) from $u = 0$ to $u = -u_{max1}$.

$$\int_0^{-u_{max1}} f_D du = \int_0^{-u_{max1}} \{-cV\sqrt{1+(u/u_{max\,1})}\}du = (2/3)cVu_{max\,1} \tag{14}$$

The energy balance law between the point of the first impulse and the point at which the maximum deformation is attained can be expressed as follows by using Equation (14).

$$mV^2/2 = k{u_{max\,1}}^2/2 + (2/3)cVu_{max\,1} \tag{15}$$

From Equation (15), u_{max1} can be obtained by

$$u_{max\,1}/d_y = \{-(4/3)h + \sqrt{(16/9)h^2+1}\}(V/V_y). \tag{16}$$

Similarly, u_{max2} can be derived. The velocity v_c at the zero restoring force timing can be obtained as follows by using the critical time interval $t_0^c = T_1'/2$ and Equation (7b).

$$v_c = V\exp(-\pi h/\sqrt{1-h^2}) \tag{17}$$

The work done by the damping force is derived by using the quadratic function approximation. The damping force-deformation relation after the second impulse is approximated by a

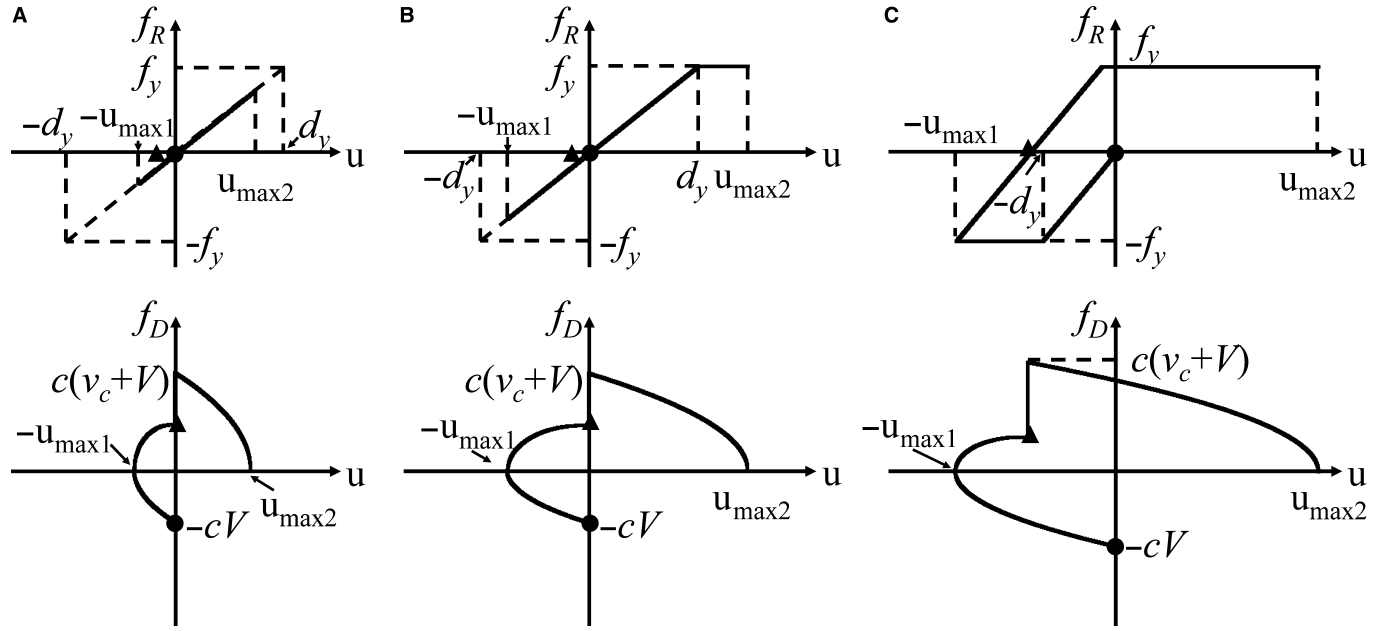

Figure 8. Evaluation of maximum elastic-plastic deformation under the critical double impulse using energy balance and quadratic approximation of the damping force-deformation relation: (A) CASE 1: elastic range, (B) CASE 2: yielding after 2nd impulse, (C) CASE 3: yielding after 1st impulse (●: 1st impulse, ▲: 2nd impulse)

quadratic function with vertex $(u, f_D) = (u_{max2}, 0)$ and passing through the point $(u, f_D) = (0, c(v_c + V))$, as shown in Figure 8A. f_D can be obtained as follows.

$$f_D = c(v_c + V)\sqrt{1 - (u/u_{max\,2})} \tag{18}$$

The work done by the damping force after the second impulse can be obtained by integrating Equation (18) from $u = 0$ to $u = u_{max2}$.

$$\begin{aligned}\int_0^{u_{max\,2}} f_D du &= \int_0^{u_{max\,2}} \{c(v_c + V)\sqrt{1 - (u/u_{max\,2})}\} du \\ &= (2/3)c(v_c + V)u_{max\,2}\end{aligned} \tag{19}$$

The energy balance law between the point of the second impulse and the point at which the maximum deformation is attained can be expressed as follows by using Equation (19).

$$m(v_c + V)^2/2 = k{u_{max\,2}}^2/2 + (2/3)c(v_c + V)u_{max\,2} \tag{20}$$

From Equations (17) and (20), u_{max2} can be obtained by

$$u_{max\,2}/d_y = \left(1 + e^{-\pi h/\sqrt{1-h^2}}\right)\left\{-(4/3)h + \sqrt{(16/9)h^2 + 1}\right\}(V/V_y) \tag{21}$$

6.3 CASE 2: Plastic deformation only after the second impulse

Second, consider CASE 2, where the system enters the yielding stage only after the second impulse. Figure 8B shows the evaluation process of the maximum deformations u_{max1},u_{max2} after the first impulse and the second impulse, respectively, in CASE 2. If the maximum deformation u_{max2} after the second impulse attains the yield deformation d_y, the system enters the plastic range after the second impulse for input that is larger than this boundary. Therefore, the boundary input velocity level between CASE 1 and CASE 2 can be obtained as follows from Equation (21) and $u_{max2} = d_y$.

$$V/V_y = \left(1 + e^{-\pi h/\sqrt{1-h^2}}\right)^{-1}\left\{(4/3)h + \sqrt{(16/9)h^2 + 1}\right\} \tag{22}$$

Since the maximum deformation just after the first impulse is in the elastic range, u_{max1} in CASE 2 is also obtained by Equation (16). u_{max2} in CASE 2 is derived in this section. The work done by the damping force in CASE 2 is derived by using the quadratic function approximation. As in CASE 1, v_c in CASE 2 can be obtained by Equation (17) due to the elastic response just after the first impulse. The work done by the damping force after the second impulse in CASE 2 can be expressed by Equation (19) by using the quadratic function approximation, as in CASE 1. The energy balance law between the point of the second impulse and the point at which the maximum deformation is attained can be expressed as follows by using Equation (19).

$$m(v_c + V)^2/2 = f_y d_y/2 + f_y(u_{max\,2} - d_y) + (2/3)c(v_c + V)u_{max\,2} \tag{23}$$

From Equations (17) and (23), u_{max2} can be obtained as

$$\frac{u_{max\,2}}{d_y} = \frac{1 + \left\{1 + \exp\left(-\pi h \Big/ \sqrt{1-h^2}\right)\right\}^2 (V/V_y)^2}{2 + (8h/3)\left\{1 + \exp\left(-\pi h \Big/ \sqrt{1-h^2}\right)\right\}(V/V_y)}. \tag{24}$$

6.4 CASE 3: Plastic deformation, even after the first impulse

Finally, consider CASE 3, where the system enters the yielding stage, even after the first impulse. Figure 8C shows the evaluation process of the maximum deformations u_{max1},u_{max2} after the first impulse and the second impulse, respectively, in CASE 3. If the maximum deformation u_{max1} after the first impulse attains the yield deformation d_y, the system enters the plastic range after the first impulse for input that is larger than

this boundary. Therefore, the boundary input velocity level between CASE 2 and CASE 3 can be obtained as follows from Equation (16) and $u_{\max 1} = d_y$.

$$V/V_y = (4/3)h + \sqrt{(16/9)h^2 + 1} \tag{25}$$

The maximum deformation $u_{\max 1}$ after the first impulse is derived. The work done by the damping force after the first impulse in CASE 3 can be expressed by Equation (14) by using the quadratic function approximation, as in CASE 1. The energy balance law between the point of the first impulse and the point at which the maximum deformation is attained can be expressed as follows by using Equation (14).

$$mV^2/2 = f_y d_y/2 + f_y(u_{\max 1} - d_y) + (2/3)cVu_{\max 1} \tag{26}$$

From Equation (26), $u_{\max 1}$ can be obtained by

$$u_{\max 1}/d_y = \{(V/V_y)^2 + 1\}/\{2 + (8h/3)(V/V_y)\} \tag{27}$$

The maximum deformation $u_{\max 2}$ after the second impulse is derived next. The velocity v_c at the zero restoring force timing after the first impulse can be obtained as follows by solving the equation of motion in the unloading process.

$$v_c = V_y \exp\left[(-h/\sqrt{1-h^2})\left\{0.5\pi + \arctan(h/\sqrt{1-h^2})\right\}\right] \tag{28}$$

The detailed derivation of Equation (28) is shown in Appendix 2. The work done by the damping force is derived by using the quadratic function approximation. The damping force-deformation relation after the second impulse is approximated by a quadratic function with vertex $(u, f_D) = (u_{\max 2}, 0)$ and passing the point $(u, f_D) = (-u_{\max 1} + d_y, -c(v_c + V))$, as shown in Figure 8C. f_D can be obtained as follows.

$$f_D = c(v_c + V)\sqrt{(u_{\max 2} - u)/(u_{\max 1} + u_{\max 2} - d_y)} \tag{29}$$

The work done by the damping force after the second impulse can be obtained by integrating Equation (29) from $u = u_{\max 1} + d_y$ to $u = u_{\max 2}$.

$$\begin{aligned}&\int_{-u_{\max 1}+d_y}^{u_{\max 2}} \{c(v_c+V)\sqrt{(u_{\max 2}-u)/(u_{\max 1}+u_{\max 2}-d_y)}\}du \\ &= (2/3)c(v_c+V)(u_{\max 1}+u_{\max 2}-d_y)\end{aligned} \tag{30}$$

The energy balance law between the point of the second impulse and the point at which the maximum deformation is attained can be expressed as follows by using Equation (30).

$$\begin{aligned}m(v_c + V)^2/2 =& f_y d_y/2 + f_y(u_{\max 1} + u_{\max 2} - 2d_y) \\ &+ (2/3)c(v_c + V)(u_{\max 1} + u_{\max 2} - d_y)\end{aligned} \tag{31}$$

From Equations (28) and (31), $u_{\max 2}$ can be obtained by

$$\begin{aligned}\frac{u_{\max 2}}{d_y} =& -\frac{u_{\max 1}}{d_y} + 1 \\ &+ \frac{\left[\frac{V}{V_y} + \exp\left\{\frac{-h}{\sqrt{1-h^2}}\left(\frac{\pi}{2} + \arctan\frac{h}{\sqrt{1-h^2}}\right)\right\}\right]^2 + 1}{2 + \frac{8h}{3}\left[\frac{V}{V_y} + \exp\left\{\frac{-h}{\sqrt{1-h^2}}\left(\frac{\pi}{2} + \arctan\frac{h}{\sqrt{1-h^2}}\right)\right\}\right]}.\end{aligned} \tag{32}$$

6.5 Maximum deformation under the critical double impulse with respect to the input velocity level

Figure 9 shows a comparison of an approximate solution for the maximum deformation $u_{\max}/d_y = \max(u_{\max 1}/d_y, u_{\max 2}/d_y)$ under the critical double impulse with respect to the input velocity level V/V_y, with the maximum deformation calculated by the time-history response analysis without the quadratic function approximation of the damping force-deformation relation. The Newmark-β method (the constant average acceleration method: $\Delta t/T_1 = 10^{-4}$) is used in the time-history response analysis, and the maximum deformation under the critical double impulse for various time intervals is calculated by changing the time interval t_0 in a parametric manner. The damping ratios $h = 0, 0.02, 0.05, 0.1, 0.2, 0.5$ are employed in Figure 9. The approximate solution with $h = 0$ is equal to the closed-form solution of the undamped system that is derived in a previous paper.[13] In comparison with the critical response that was obtained by the time-history response analysis, the approximate closed-form solution that was derived in Sections 6.2-6.4 can simulate the elastic-plastic response of the system with viscous damping under the critical double impulse with reasonable accuracy, except when $V/V_y > 3$ in the model with $h = 0.2, 0.5$. The region in which $u_{\max 2} > u_{\max 1}$ is satisfied decreases as the damping ratio increases.

Figure 10 shows the critical time interval t_0^c that was calculated by time-history response analysis with respect to the input velocity level. The closed-form expression of the critical time interval t_0^c of the undamped system was derived by solving the equation of motion in the previous paper.[13] Since it is difficult to derive the critical time interval for the system with viscous damping by solving the equation of motion, the critical time interval is obtained here by using time-history response analysis. From Figure 10, the time interval becomes shorter as the damping ratio increases at the input velocity level at which the system enters the plastic region.

Figure 11 shows a comparison of the restoring force deformation relation and the damping force-deformation relation that were obtained by using the quadratic function approximation with those that were obtained by time-history response analysis. $h = 0.05$ is employed and Figures 11A-C present the comparisons for $V/V_y = 0.4$ in CASE 1, $V/V_y = 0.8$ in CASE 2, and $V/V_y = 2.0$ in CASE 3, respectively. According to Figure 11, the damping force-deformation relation can be approximated properly by a quadratic function.

Figure 12 shows $u_{\max 2}/u_{\max 2}^c$ with respect to the varying time interval t_0 and the restoring force at the time $t = t_0$ after the first impulse for $V/V_y = 2.0$, $h = 0.05$, obtained by time-history response analysis. In Figure 12, $u_{\max 2}$ and $u_{\max 2}^c$ denote the maximum deformations after the second impulse under the double impulse with the varying time interval and under the critical double impulse (the maximum value of $u_{\max 2}$), respectively. $u_{\max 2}$ and $u_{\max 2}^c$ are calculated by time-history response analysis. One of the ordinates of Figure 12 denotes $u_{\max 2}$, normalized by $u_{\max 2}^c$, and the other denotes the restoring force f at $t = t_0$, normalized by the yield force f_y. According to Figure 12, the restoring force becomes zero at the time $t = t_0$ at which $u_{\max 2}$ reaches $u_{\max 2}^c$. Therefore, the zero restoring force timing after the first impulse is the critical timing of the second impulse of the SDOF elastic-perfectly plastic system with viscous damping.

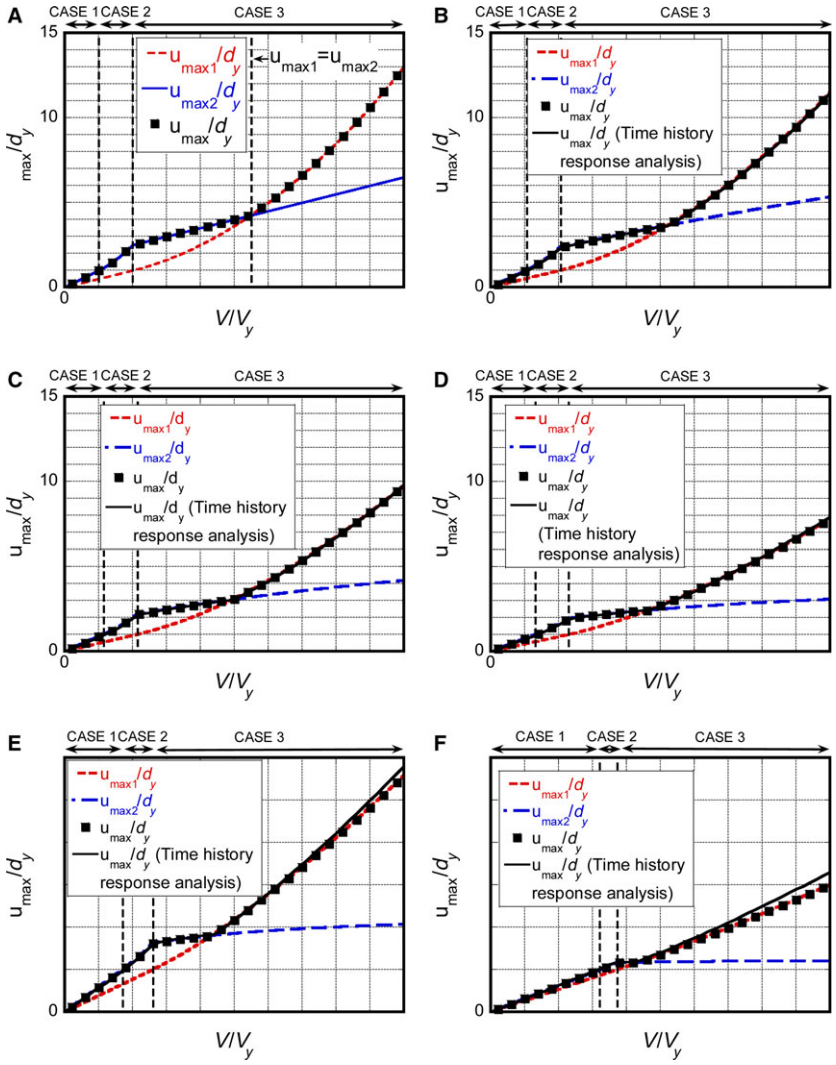

Figure 9. Comparison of the maximum elastic-plastic deformation u_{max}/d_y of the model with viscous damping under the critical double impulse using the quadratic approximation of the damping force-deformation relation with that obtained by time-history response analysis: (A) $h = 0$[13], (B) $h = 0.02$, (C) $h = 0.05$, (D) $h = 0.1$, (E) $h = 0.2$, (F) $h = 0.5$

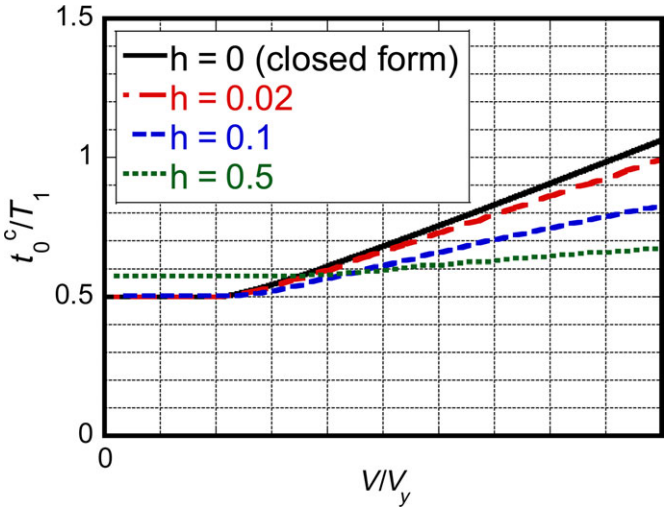

Figure 10. Critical impulse timing t_0^c/T_1 for varied input level V/V_y in models with various damping ratios

7. Accuracy check by time-history response analysis to the one-cycle sinusoidal wave

To check the accuracy of using the double impulse as a substitute for the one-cycle sinusoidal wave in representing the fling-step near-fault ground motions, time-history response analysis of the SDOF elastic-perfectly plastic system with viscous damping under the one-cycle sinusoidal wave is conducted. The maximum velocity V_p of the corresponding one-cycle sinusoidal wave is adjusted so that the maximum Fourier amplitude of the one-cycle sinusoidal wave is equal to that of the double impulse.[13,15,16] Equation (3) is used as an acceleration waveform of the one-cycle sinusoidal wave. The period T_p of the one-cycle sinusoidal wave is $T_p = 2t_0^c$, where t_0^c is calculated by time-history response analysis, as shown in Figure 10.

Figure 13 shows a comparison of the maximum deformation of the SDOF elastic-perfectly plastic system with viscous damping under the critical double impulse with that under the corresponding one-cycle sinusoidal wave for the damping ratios $h = 0,0.02,0.05,0.1,0.2,0.5$. The maximum deformation of the undamped system under the critical double impulse is in

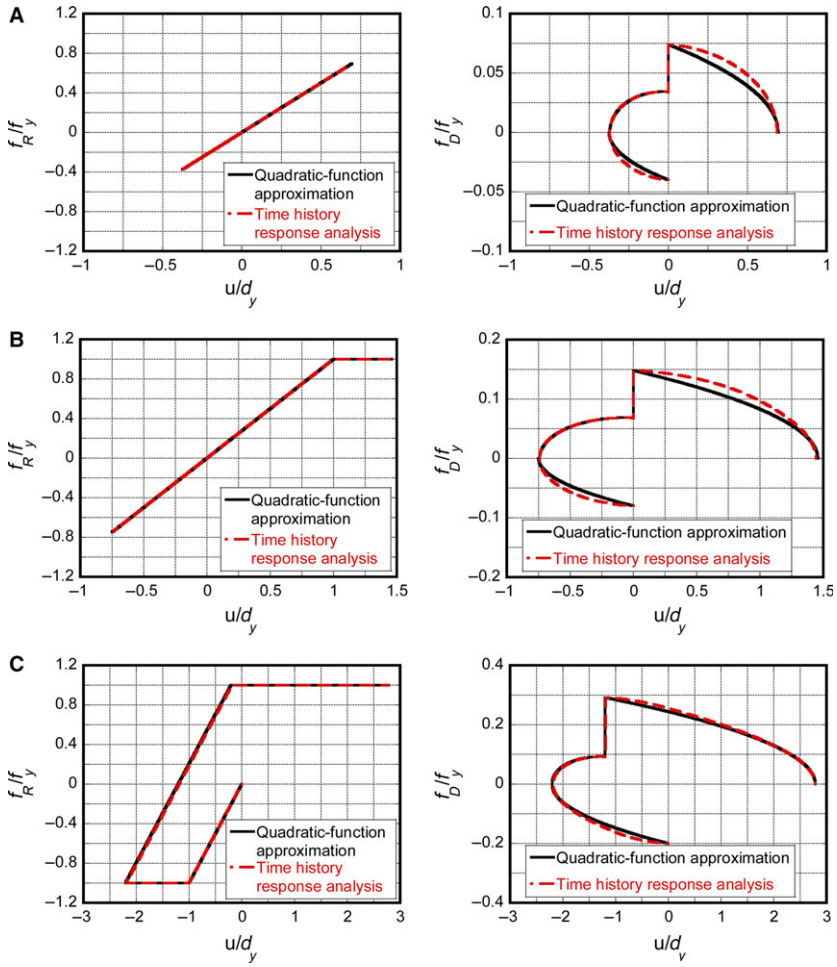

Figure 11. Comparison of elastic-plastic responses under the critical double impulse that were obtained using quadratic approximation of damping force-deformation relation with those that were obtained by time-history response analysis (h = 0.05): (A) V/V_y = 0.4, (B) V/V_y = 0.8, (C) V/V_y = 2.0

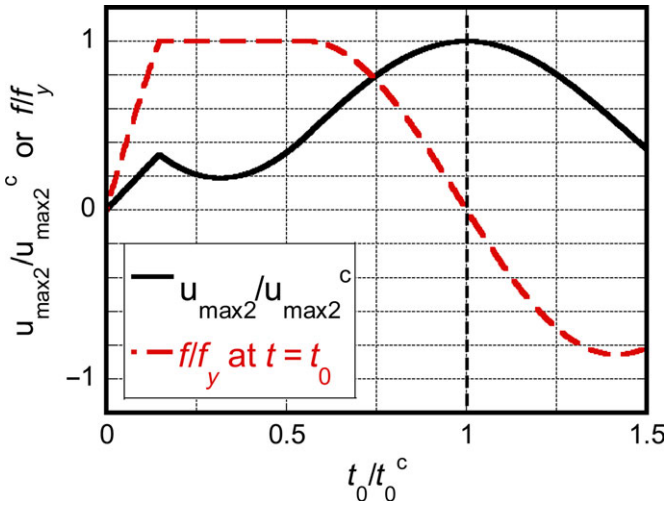

Figure 12. Maximum deformation after the 2nd impulse u_{max2}/d_y and restoring force f/f_y at $t = t_0$ for t_0/t_0^c (V/V_y = 2.0, h = 0.05)

good agreement with that under the one-cycle wave in the range of the input velocity level $V/V_y < 3$. As the damping ratio increases, the maximum deformation under the critical double impulse corresponds to that under the one-cycle sinusoidal wave in a wider range of input velocity level. This is because the maximum deformation after the first impulse exhibits better correspondence with that under the first half-cycle of the corresponding one-cycle sinusoidal wave as the damping ratio increases. The adjustment method of the input level of the double impulse and the corresponding one-cycle sinusoidal wave based on the equivalence of the maximum Fourier amplitude is appropriate for the elastic-plastic system with viscous damping.

8. Applicability of the proposed theory to actual recorded ground motion

The applicability of the proposed theory to actual recorded ground motion is investigated through the comparison of the critical elastic-plastic response under the near-fault ground motion with the elastic-plastic response under the critical double impulse. The Rinaldi station fault-normal component during the Northridge earthquake in 1994 and the Kobe

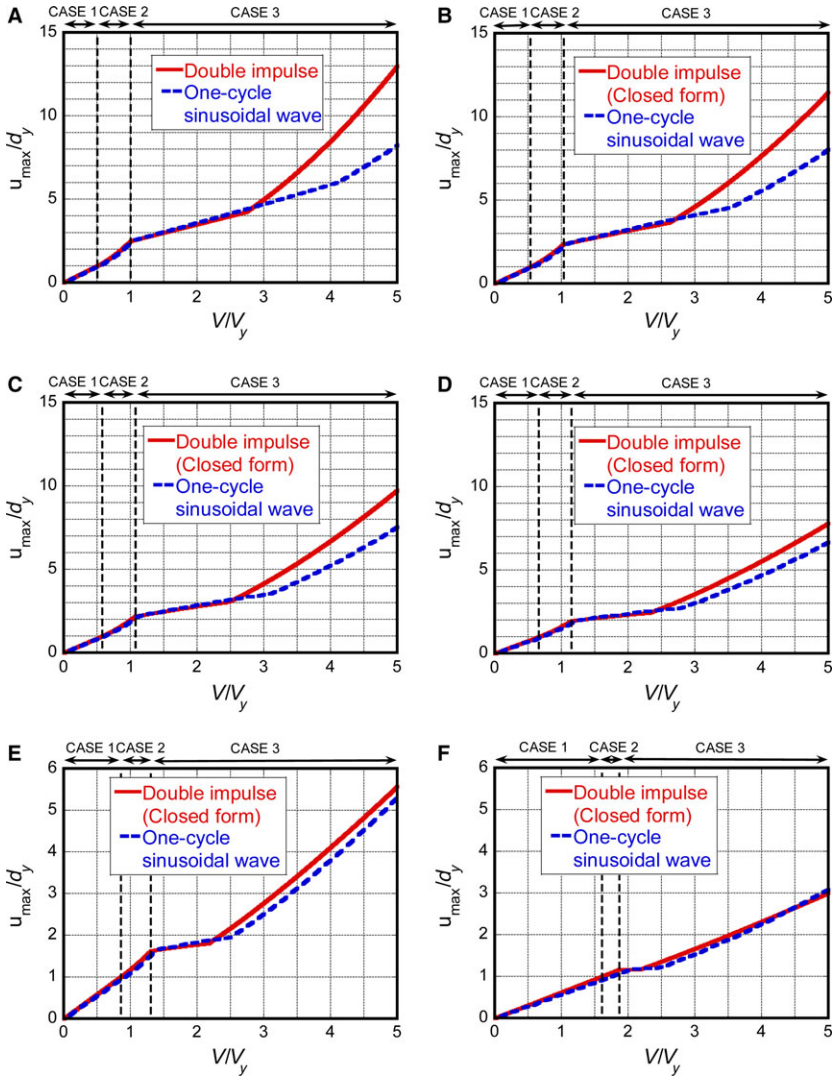

Figure 13. Comparison of the maximum elastic-plastic deformation u_{max}/d_y of the model with viscous damping under critical double impulse (quadratic function approximation) with that under the equivalent one-cycle sine wave: (A) $h = 0$,[13] (B) $h = 0.02$, (C) $h = 0.05$, (D) $h = 0.1$, (E) $h = 0.2$, (F) $h = 0.5$

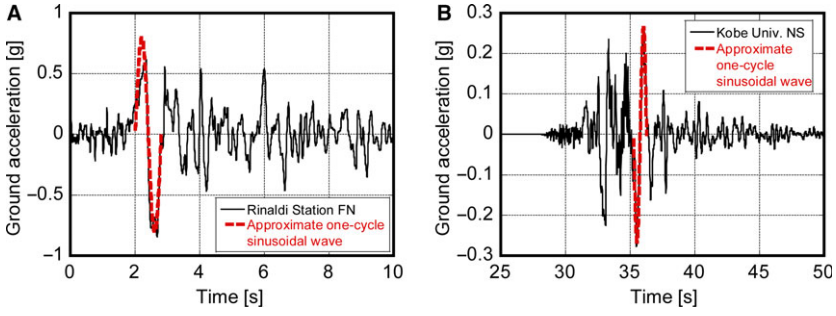

Figure 14. Recorded near-fault ground motion and corresponding one-cycle sine wave: (A) Rinaldi Station FN comp. (Northridge 1994), (B) Kobe Univ. NS comp. (Hyogoken-Nanbu 1995)

University NS component (almost fault-normal) during the Hyogoken-Nanbu (Kobe) earthquake in 1995 are used as the near-fault ground motions. The accelerograms of these two ground motions are shown in Figure 14. Although these are the fault-normal ground motions, these are represented by the double impulse in this paper. The main part of the recorded ground motion acceleration is modeled as a one-cycle sinusoidal wave, as shown in Figure 14, and the one-cycle sinusoidal wave is substituted by the double impulse by using the method shown in Section 2.

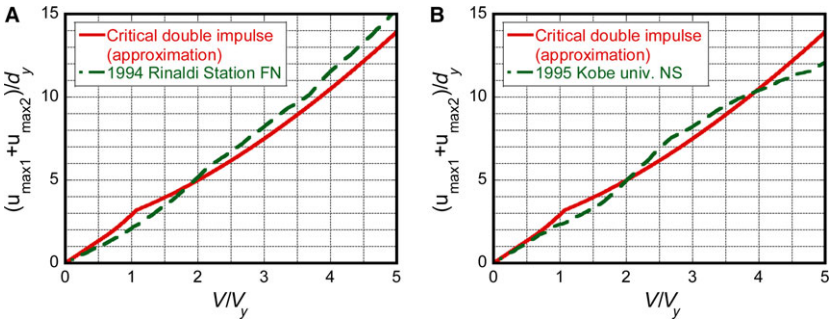

Figure 15. Comparison of the maximum elastic-plastic deformation (double amplitude) of the model with viscous damping (h = 0.05) under critical double impulse (quadratic function approximation) and the recorded ground motion: (A) Rinaldi Sta. FN comp., (B) Kobe Univ. NS comp.

Although the critical double impulse is determined for a given structural parameter V_y in Section 6, the structural parameter is selected to approximately maximize the response for a given input velocity V of the actual recorded ground motion in this section. This procedure is similar to the elastic-plastic response spectrum (changing the strength parameter), which was developed in 1960-1970.[21] In this paper, a method for evaluating the critical elastic-plastic response under the near-fault ground motion that is used in the literature[16] is employed. The input velocity level of the Rinaldi station fault-normal component is V = 1.64[m/s] and that of the Kobe University NS component is V = 0.677[m/s] by the method in the literature.[16]

Figures 15A and B show a comparison of the critical elastic-plastic response under the Rinaldi station fault-normal component and the Kobe University NS component with the proposed closed-form expression of the elastic-plastic response under the critical double impulse. The ordinate presents the maximum amplitude of deformation (the sum of u_{max1} and u_{max2}), and the abscissa is the input velocity level V/V_y. In comparison with the undamped case shown in figures 15a and 16a in the literature,[16] the elastic-plastic response under the critical double impulse corresponds well to the critical elastic-plastic response under the actual recorded ground motion in a wide range of the input velocity level, owing to the existence of viscous damping.

9. Conclusions

The double impulse was introduced as a substitute for the one-cycle sinusoidal wave in representing the main part of a near-fault ground motion. A closed-form expression was derived for the maximum deformation of the SDOF elastic-perfectly plastic system with viscous damping under the critical double impulse. The detailed conclusions are summarized as follows:

(1) A closed-form solution was derived approximately for the maximum deformation of the SDOF elastic-perfectly plastic system with viscous damping under the critical double impulse. It is difficult to obtain the exact analytical solution of the response of the elastic-plastic system with viscous damping by solving the differential equation, even by using the double impulse. Therefore, an approximate closed-form solution for the critical response of the system with viscous damping was proposed by using (i) a quadratic function that approximates the damping force-deformation relation, (ii) the assumption that the zero restoring force timing is the critical timing of the second impulse, and (iii) the energy balance law for the elastic-plastic system with viscous damping. By using the proposed method, an approximate critical response of the elastic-plastic system with viscous damping under the double impulse can be evaluated efficiently.

(2) The accuracy of the quadratic function approximation of the damping force-deformation relation and the validity of the assumption on the critical timing were investigated by using time-history response analysis. Through comparison with the result of the time-history response analysis, the damping force-deformation relation can be approximated by a quadratic function with reasonable accuracy. According to the investigation in which a variable time interval was considered, the zero restoring force timing is the critical timing of the second impulse, which maximizes the peak deformation after the second impulse.

(3) The validity of using the double impulse as a substitute for the near-fault ground motion was investigated through the comparison with the elastic-plastic response under the corresponding one-cycle sinusoidal wave. Although the response of the undamped system under the critical double impulse does not exhibit good correspondence with that under the corresponding one-cycle sinusoidal wave in the range of the larger input velocity level $V/V_y > 3$, the maximum deformation of the system with larger viscous damping under the critical double impulse corresponds well to that under the corresponding one-cycle sinusoidal wave, even in the range of the larger input velocity level.

(4) The applicability of the proposed method using the critical double impulse (defined in Section 6) to actual earthquake ground motions was investigated through comparison with the critical elastic-plastic response under actual recorded ground motions. The elastic-plastic response of the system with viscous damping under the critical double impulse corresponds well to the critical elastic-plastic response under the recorded near-fault ground motions in the wider range of the input velocity level, in comparison with the undamped system.

Acknowledgements

This support by funders is greatly appreciated. Part of this work is supported by the Grant-in-Aid for Scientific Research (KAKENHI) of Japan Society for the Promotion of Science (nos'. 5H04079, 15J00960) and Sumitomo Rubber Industries, Co.

Disclosure

The authors have no conflict of interest to declare.

Appendix 1: Critical impulse timing for the linear elastic system with viscous damping

The critical timing of the second impulse for a linear elastic system with viscous damping is explained. The maximum deformation u_{max2} after the second impulse for a variable impulse time interval can be obtained by Equation (10b). u_{max2} is maximized at the time interval at which the derivative of Equation (10b) with respect to the time interval t_0 becomes zero. From Figure 5, the maximum value of u_{max2} decreases due to the effect of viscous damping as the time interval becomes longer. Therefore, the maximum value of u_{max2} is investigated in the range $0 < t_0 < T_1'$. However, it is complicated to obtain the derivative of Equation (10b) with respect to the time interval t_0. In a simple manner, $t_0 = T_1'/2$ is substituted into the equation of du_{max2}/dt_0. It is confirmed that du_{max2}/dt_0 is zero at that value. t_{max2},ϕ,θ in Equation (10b) can be obtained from Equations (9a), (9b), (11a), and (11b), respectively. It is noted that t_{max2} and θ are functions of t_0.

Appendix 2: Velocity at zero restoring force after attaining u_{max1} in CASE 3

The velocity at the zero restoring force timing after the first impulse in CASE 3 can be obtained by solving the equation of motion in the unloading process. An outline of the derivation of v_c is shown here. The restoring force characteristic can be obtained as follows by using u_{max1}.

$$f_R = ku + k(u_{max\,1} - d_y), \tag{A1}$$

where an approximate solution of u_{max1} is obtained from Equation (27). The equation of motion (free vibration) in the unloading process can be expressed by using Equation (A1).

$$m\ddot{u} + c\dot{u} + ku + k(u_{max\,1} - d_y) = 0 \tag{A2}$$

From Equation (A2), the deformation and velocity in the unloading process can be obtained by

$$u = -(1/\sqrt{1-h^2})d_y e^{-h\omega_1 t}\cos(\omega_1' t - \phi) - (u_{max\,1} - d_y), \tag{A3}$$

$$\dot{u} = (1/\sqrt{1-h^2})V_y e^{-h\omega_1 t}\sin(\omega_1' t), \tag{A4}$$

where the starting time of the unloading process (the point $-u_{max1}$ in Figure 8C) is taken as $t = 0$. ϕ is obtained from Equation (9a). From Equations (A1) and (A3), the time t^c at which the restoring force becomes zero can be obtained as follows.

$$t^c = \left[0.25 + \{\arctan(h/\sqrt{1-h^2})\}/(2\pi)\right]T_1' \tag{A5}$$

v_c can then be obtained by substituting Equation (A5) into Equation (A4).

$$v_c = V_y \exp\left[(-h/\sqrt{1-h^2})\{0.5\pi + \arctan(h/\sqrt{1-h^2})\}\right] \tag{A6}$$

References

1 Sasani M, Bertero VV. Importance of severe pulse-type ground motions in performance-based engineering: historical and critical review. Proceedings of the Twelfth World Conference on Earthquake Engineering, Auckland, New Zealand, 2000.
2 Hisada Y. Evaluation of the Input Ground Motion of the Revised Seismic Code 2000 Considering the Characteristics of Near-Source Strong Ground Motions. The 29th Symposium of Earthquake Ground Motion, The Architectural Institute of Japan, pp. 99-110, 2001 (in Japanese).
3 Mavroeidis GP, Papageorgiou AS. A mathematical representation of near-fault ground motions. *Bull Seism Soc Am*. 2003;**93**:1099-1131.
4 Makris N, Black CJ. Dimensional analysis of rigid-plastic and elastoplastic structures under pulse-type excitations. *J Eng Mech ASCE*. 2004;**130**:1006-1018.
5 Mavroeidis GP, Dong G, Papageorgiou AS. Near-fault ground motions, and the response of elastic and inelastic single-degree-freedom (SDOF) systems. *Earthquake Eng Struct Dyn*. 2004;**33**:1023-1049.
6 Kalkan E, Kunnath SK. Effects of fling step and forward directivity on seismic response of buildings. *Earthquake Spectra*. 2006;**22**:367-390.
7 Khaloo AR, Khosravi H, Hamidi Jamnani H. Nonlinear interstory drift contours for idealized forward directivity pulses using "Modified Fish-Bone" models. *Adv Struct Eng*. 2015;**18**:603-627.
8 Minami H, Hayashi Y. Response characteristics evaluation of elastic shear beam for pulse waves. *J Struct Constr Eng AIJ*. 2013;**78**:453-460. (in Japanese).
9 Sakai Y, Minami T, Kabeyasawa T. A method to simplify strong ground motion to a 1 cycle sine wave by taking into account inelastic responses of structures. *J Struct Eng AIJ*. 1999;**45B**:81-86. (in Japanese).
10 Yamada K. Maximum displacement response of 1 DOF system subjected to 1 cycle sine wave. *AIJ J Technol Des*. 2002;**8**:63-66. (in Japanese).
11 Ogawa K. Earthquake input energy during half-cycle of vibration and maximum seismic response of bilinear systems. *J Struct Constr Eng AIJ*. 2000;**65**:185-192. (in Japanese).
12 Miyaji S, Ogawa K. Prediction of maximum inter-story drift angles in conventional braced steel frames. *J Struct Constr Eng AIJ*. 2014;**79**:1175-1182. (in Japanese).
13 Kojima K, Takewaki I. Critical earthquake response of elastic-plastic structures under near-fault ground motions (Part 1: Fling-step input). *Front Built Environ*. 2015;**1**:12.
14 Kojima K, Takewaki I. Critical earthquake response of elastic-plastic structures under near-fault ground motions (Part 2: Forward-directivity input). *Front Built Environ*. 2015;**1**:13.
15 Kojima K, Takewaki I. Closed-form critical earthquake response of elastic-plastic structures on compliant ground under near-fault ground motions. *Front Built Environ (Specialty Section: Earthquake Engineering)*. 2016;**2**:1.
16 Kojima K, Talewaki I. Closed-form critical earthquake response of elastic-plastic structures with bilinear hysteresis under near-fault ground motions. *J Struct Constr Eng AIJ*. 2016;**81**:1209-1219. (in Japanese).
17 Drenick RF. Model-free design of aseismic structures. *J Eng Mech Div ASCE*. 1970;**96(EM4)**:483-493.
18 Takewaki I. *Critical Excitation Methods in Earthquake Engineering*. Amsterdam: Elsevier; 2007.
19 Caughey TK. Sinusoidal excitation of a system with bilinear hysteresis. *J Appl Mech*. 1960;**27**:640-643.
20 Iwan WD. The dynamic response of bilinear hysteretic systems. PhD Thesis, California Institute of Technology, 1961.
21 Veletsos AS, Newmark NM, Chelapati CV. Deformation spectra for elastic and elasto-plastic systems subjected to ground shock and earthquake motions. Proceedings of the Third World Conference on Earthquake Engineering, New Zealand, Vol. II, pp. 663-682, 1965.

How to cite this article: Kojima K, Saotome Y, Takewaki I. Critical earthquake response of a SDOF elastic-perfectly plastic model with viscous damping under double impulse as a substitute for near-fault ground motion. *Jpn Archit Rev*. 2018;1:207–220. https://doi.org/10.1002/2475-8876.10019